NONLINEAR BANG-BANG IMPACT CONTROL USING TIME DELAY: STABILITY ANALYSIS AND EXPERIMENTS

***Sang-Hoon Kang, *Pyung H. Chang, *Maolin Jin, **Eunjeong Lee**

**Department of Mechanical Engineering*
***Department of Electrical Engineering and Computer Science*
Korea Advanced Institute of Science and Technology
373-1 Guseong-dong, Yuseong-gu, Daejeon 305-701, Republic of Korea
e-mail:{ sh_kang , phchang , mulan819} @.kaist.ac.kr,** eunjeonglee@ieee.org*

Abstract: This paper presents stability analysis of the nonlinear bang-bang impact control for multi degree of freedom robotic manipulators based on the analysis in L_∞^n space. The physical implication of sufficient stability conditions are explained in terms of sampling time, accuracy of inertia estimation, control gains, and the rate of change in the Coriolis, centrifugal and disturbance forces. The stability conditions are verified by experiments.

Keywords: stability criteria, impedance control, force control, Bang-bang control, time-delay estimation, robots.

1. INTRODUCTION

It has been known to be very difficult for robots to interact with a variety of environments including stiff one with one simple control algorithm and gain (Indri, and Tornambe, 1999; Nenchev, and Yoshida, 1999).

In order to address this problem, a nonlinear bang-bang impact control (NBBIC) has been proposed by Lee (Lee, 1994; Lee, *et al*., 2003a, b). Under NBBIC, a robot can successfully interact with an environment without changing control algorithm and control gains throughout all three modes: free space, transition and constrained motion. Experiments show that overall performance of NBBIC is superior or comparable to more complicated existing impact force control techniques (Lee, 1994; Lee, *et al*., 2003a, b). However, a formal presentation of stability analysis has not been made yet.

In this paper, stability analysis of the nonlinear bang-bang impact control is presented for multi degree of freedom robotic manipulators. Sufficient stability conditions have been derived based on the analysis in L_∞^n space and their physical interpretation has been given.

This paper is organized as follows: Section 2 describes hybrid Natural Admittance/Time-Delay Control (NAC/ TDC) with the proposed bang-bang impact control. Section 3 presents the stability analysis of the NBBIC and discusses its physical implications, while Section 4 validates the NBBIC stability theorem through experiment and discusses noise effects. Section 5 discusses conclusions and suggestions for future work

2. NONLINEAR BANG-BANG IMPACT CONTROL

In this section, the hybrid NAC/TDC is presented (Lee, 1994; Lee, *et al*., 2003a, b), and a nonlinear bang-bang impact control strategy is explained for stability analysis (Lee, 1994; Lee, *et al*., 2003a, b).

2.1 Hybrid Natural Admittance/Time Delay Control

Hybrid Natural Admittance/Time Delay Control (NAC/TDC) is developed to enhance the robustness of NAC against modelling uncertainty and disturbance via time delay estimation (Lee, 1994; Lee, *et al*., 2003a, b). NAC obtains maximum target admittance within passivity constraint

Let us consider the nonlinear dynamics of n degree of freedom robots

$$\boldsymbol{\tau}(t)=\mathbf{M}(\boldsymbol{\theta}(t))\ddot{\boldsymbol{\theta}}(t)+\mathbf{V}(\boldsymbol{\theta}(t),\dot{\boldsymbol{\theta}}(t))+\mathbf{g}(\boldsymbol{\theta}(t))+\boldsymbol{\tau}_s(t)+\mathbf{d}(t)\,,\quad(1)$$

where $t\in\Re$ represents time. $\boldsymbol{\theta}(t)\in\Re^n$ and $\dot{\boldsymbol{\theta}}(t)\in\Re^n$ represents joint angle and velocity vector, respectively. $\mathbf{M}(\boldsymbol{\theta}) \in \Re^{n\times n}$, $\mathbf{V}(\boldsymbol{\theta},\dot{\boldsymbol{\theta}})$, $\mathbf{G}(\boldsymbol{\theta}) \in \Re^{n}$, and $\mathbf{d}(t) \in \Re^{n}$ are an inertia matrix, Coriolis and centrifugal force vector, gravitational force vector, and the disturbance vector which includes viscous and Coulomb friction and external disturbances, respectively. $\boldsymbol{\tau}_s, \boldsymbol{\tau}(t) \in \Re^{n}$ are the external torque vector measured and the control torque vector applied to the joints, respectively.

The simplest form of NAC/TDC (Lee, 1994; Lee, *et al.*, 2003a, b) for the *n* degree of freedom robot above is

$$\boldsymbol{\tau}(t)=\bar{\mathbf{M}}\left[\mathbf{G}_v\left(\dot{\boldsymbol{\theta}}_{cmd}-\dot{\boldsymbol{\theta}}\right)+\mathbf{K}_{des}\mathbf{e}+\mathbf{B}_{des}\dot{\mathbf{e}}+\mathbf{c}_r\boldsymbol{\theta}\right]-\bar{\mathbf{M}}\ddot{\boldsymbol{\theta}}(t-L)+\boldsymbol{\tau}(t-L), \quad (2)$$

where

$$\dot{\boldsymbol{\theta}}_{cmd}(t)=\int M_s^{-1}\left\{\boldsymbol{\tau}_s+\mathbf{K}_{des}(\boldsymbol{\theta}_{des}(t)-\boldsymbol{\theta}(t))+\mathbf{B}_{des}(\dot{\boldsymbol{\theta}}_{des}(t)-\dot{\boldsymbol{\theta}}(t))\right\}dt \quad (3)$$

L is a small time-delay and can be regarded as a sampling time. $\boldsymbol{\theta}_{des}(t), \dot{\boldsymbol{\theta}}_{des}(t) \in \Re^{n}$, and $\dot{\boldsymbol{\theta}}_{cmd}(t) \in \Re^{n}$ are desired joint position, velocity and the command joint velocity vector, respectively. $\bar{\mathbf{M}} \in \Re^{n\times n}$ is a constant matrix representing the inertia estimate. $M_s \in \Re$ and $\mathbf{c}_r \in \Re^{n\times n}$ are the end-point mass obtained by system identification and the negative-definite constant position-feedback-gain matrix, respectively (Youcef-Toumi, and Ito, 1990). $\mathbf{G}_v, \mathbf{K}_{des}, \mathbf{B}_{des} \in \Re^{n\times n}$ are the diagonal constant velocity-feedback-gain matrix and the desired stiffness and damping matrices, respectively.

In order to implement the control law only one system parameter, the inertia, needs to be estimated. The effect of measurement noise does not seriously affect system performance of NAC/TDC (Lee, 1994; Lee, *et al.*, 2003b), since in discrete form TDC is equivalent to PID control and joint acceleration term turns into joint velocity term (Lee, *et al.*, 1997).

2.2 Nonlinear Bang-Bang Impact Control

Even though the NAC/TDC yields good control performance during free and constrained motion, its performance is limited when a robot experiences impact. Therefore, a nonlinear bang-bang impact controller is proposed to enhance the impact behavior of robots by using the NAC/TDC (Lee, 1994; Lee, *et al.*, 2003a, b). The control strategy can be summarized as follows. During free-space motion, NAC/TDC is used. During impact transient when contact is broken due to bouncing, no control input is applied; and when contact is made, NAC/TDC is used. NAC/TDC is used again after contact is established. NAC/TDC also brings a robot back into contact with an environment when it stops in free space due to the zero control input during contact transient. This incident occurs if the restoring spring force cannot overcome friction and inertia of the robot under no control action after it bounces off from the environment. The resulting control strategy for a multi-input multi-output (MIMO) system is described as follows.

1) Unconstrained Motion: NAC/TDC
   If $|\mathbf{F}_s| < F_{impact}$, then NAC/TDC (4)

2) In contact Transition: Bang-Bang Control
   a) If the robot is in contact with the environment ($|\mathbf{F}_s| > F_{sw}$), then NAC/TDC (5)
   b) If the robot is out of contact ($|\mathbf{F}_s| < F_{sw}$), then $\boldsymbol{\tau}(t)=0$ (6)
   c) If $|\mathbf{F}_s| < F_{sw}$ and $|\mathbf{v}(t)| < v_{threshold}$, then NAC/TDC (7)

3) After Impact Transient: NAC/TDC
   If $|\mathbf{F}_s| > F_{sw}$, then NAC/TDC (8)

$\mathbf{F}_s, \mathbf{v} \in \Re^{n}$ are sensed force and Cartesian velocity respectively. F_{impact}, $F_{sw} \in \Re$ *and* $v_{threshold} \in \Re$ are threshold values to detect impact, switching and zero velocity, respectively, and are dependent on the sensitivity of the torque and position sensors. These values should be zero ideally, but they have certain threshold values in reality due to experimental noises. The NBBIC is very effective since it makes robots naturally dissipate their impact energy after they bounce off from the environment rather than exert excessive control input to reject impact disturbance.

3. STABILITY ANALYSIS OF NONLINEAR BANG-BANG IMPACT CONTROL

3.1 Grouping of Each Control Stage

For stability analysis, the five stages, (4)-(8), have been categorized into three groups in table 1 according to their physical characteristics and contact mode. The stability analysis was performed for each group separately. The stability condition for the transition from one group to the next can be derived from that of the next group it switched to by setting nonzero initial condition. Finite number of switching is guaranteed because velocity is reduced to a small value that cannot make bounce after 2nd impact (Appendix).

3.2 NAC/TDC Error-ε Inequality

In order to derive the stability condition of NBBIC, we first established the general inequality for NAC/TDC. The nonlinear dynamics of (1) for *n* degree of freedom robot can be divided into two terms, the known term and the unknown and/or uncertain nonlinear dynamics terms represented by $\mathbf{H}(t) \in \Re^{n}$ as below.

$$\boldsymbol{\tau}(t) = \bar{\mathbf{M}}\ddot{\boldsymbol{\theta}}(t) + \mathbf{H}(t), \quad (9)$$

where

$$\mathbf{H}(t)=\left(\mathbf{M}(\boldsymbol{\theta}(t))-\bar{\mathbf{M}}\right)\ddot{\boldsymbol{\theta}}(t)+\mathbf{V}(\boldsymbol{\theta}(t),\dot{\boldsymbol{\theta}}(t))+\mathbf{G}(\boldsymbol{\theta}(t))+\mathbf{d}(t)+\boldsymbol{\tau}_s(t). \quad (10)$$

Likewise, the NAC/TDC of (2)can be described as follows.

$$\boldsymbol{\tau}(t) = \bar{\mathbf{M}}\mathbf{u}(t) + \mathbf{H}(t-L), \quad (11)$$

Table 1 Grouping of control Stage

Group	Characteristics: Physical Characteristics	Characteristics: Mode	Case
Group 1	- Before Contact - No external force	Free space - 1	1 2-c
Group 2	- Nonzero external force	Constrained space	2-a,3
Group 3	- Out of contact - No external force	Free space - 2	2-b
	$\mathbf{e}(0) \neq 0$, $\dot{\mathbf{e}}(0) \neq 0$, $\ddot{\mathbf{e}}(0) \neq 0$		All cases

where

$$\mathbf{u}(t)=\mathbf{G}_v(\dot{\boldsymbol{\theta}}_{cmd}(t)-\dot{\boldsymbol{\theta}}(t))+\mathbf{K}_{des}\mathbf{e}(t)+\mathbf{B}_{des}\dot{\mathbf{e}}(t)+\mathbf{c}_r\boldsymbol{\theta}(t) \quad (12)$$

where

$$\dot{\boldsymbol{\theta}}_{cmd}(t)=\int M_s^{-1}\left\{\boldsymbol{\tau}_s+\mathbf{K}_{des}(\boldsymbol{\theta}_{des}(t)-\boldsymbol{\theta}(t))+\mathbf{B}_{des}(\dot{\boldsymbol{\theta}}_{des}(t)-\dot{\boldsymbol{\theta}}(t))\right\}dt . \quad (13)$$

Subtracting (11) from (9) yields,

$$\bar{\mathbf{M}}(\mathbf{u}(t)-\ddot{\boldsymbol{\theta}}(t))=\mathbf{H}(t)-\mathbf{H}(t-L) \cdot \quad (14)$$

If we set

$$\boldsymbol{\varepsilon}(t)\equiv\mathbf{u}(t)-\ddot{\boldsymbol{\theta}}(t), \quad (15)$$

then (15) can be written as below.

$$\boldsymbol{\varepsilon}(t)=\bar{\mathbf{M}}^{-1}\left(\mathbf{H}(t)-\hat{\mathbf{H}}(t)\right)=\bar{\mathbf{M}}^{-1}\left(\mathbf{H}(t)-\mathbf{H}(t-L)\right) \quad (16)$$

$\boldsymbol{\varepsilon}(t)\in\Re^n$ is an estimation error vector between the nonlinear dynamics $\mathbf{H}(t)$ and the estimated nonlinear dynamics $\hat{\mathbf{H}}(t)$. $\hat{\mathbf{H}}(t)$ is estimated by using $\mathbf{H}(t-L)$, the value of nonlinear dynamics at time *t-L*.

The substitution of (12) and (3) into (15) and mathematical manipulation yields the following error dynamics. The mathematical manipulation does not necessitate the initial value of $\dot{\theta}_{cmd}$.

$$\begin{aligned} &M_s^{-1}\mathbf{G}_v\mathbf{K}_{des}\int\mathbf{e}(t)dt+\left(M_s^{-1}\mathbf{G}_v\mathbf{B}_{des}+\mathbf{K}_{des}-\mathbf{c}_r\right)\mathbf{e}(t)\\ &+\left(\mathbf{G}_v+\mathbf{B}_{des}\right)\dot{\mathbf{e}}(t)+\ddot{\mathbf{e}}(t)\\ &=\boldsymbol{\varepsilon}(t)-\mathbf{c}_r\boldsymbol{\theta}_{des}(t)+\ddot{\boldsymbol{\theta}}_{des}(t)+\mathbf{G}_v\dot{\boldsymbol{\theta}}_{des}(t)-M_s^{-1}\mathbf{G}_v\int\boldsymbol{\tau}_s dt \end{aligned} \quad ,(17)$$

where $\mathbf{e}(t)=\boldsymbol{\theta}_{des}(t)-\boldsymbol{\theta}(t)$. Equation (17) describes the time-delay estimation error $\boldsymbol{\varepsilon}(t)$ in terms of the desired trajectories and the errors between the desired trajectories and the actual plant states and their derivatives.

Lemma1.Error-ε Inequality: In the case of n degree of freedom robot under NAC/TDC in constrained space, if the desired trajectory and its derivatives are in L_∞^n space and the external force $\boldsymbol{\tau}_s$ is in L_∞^n space, i.e., $\boldsymbol{\theta}_{des}(t),\dot{\boldsymbol{\theta}}_{des}(t)\in L_\infty^n$, $\ddot{\boldsymbol{\theta}}_{des}(t)\in L_\infty^n$ and $\boldsymbol{\tau}_s\in L_\infty^n$, then the following inequalities can be obtained. In the case of impact, $\boldsymbol{\tau}_s\in L_\infty^n$ holds because $\|\boldsymbol{\tau}_s\|_\infty=\sup_{t>0}|\delta_a(t)|=1/2a$. $\delta_a(t)$ is the unit pulse function[1].

$$\begin{aligned} \|\mathbf{e}\|_{T\infty}&\le\beta_1\|\boldsymbol{\varepsilon}\|_{T\infty}+\gamma_1\|\boldsymbol{\tau}_s\|_{T\infty}+\eta_1\|\boldsymbol{\theta}_{des}\|_{T\infty}+\rho_1\\ \|\dot{\mathbf{e}}\|_{T\infty}&\le\beta_2\|\boldsymbol{\varepsilon}\|_{T\infty}+\gamma_2\|\boldsymbol{\tau}_s\|_{T\infty}+\eta_2\|\dot{\boldsymbol{\theta}}_{des}\|_{T\infty}+\rho_2\\ \|\ddot{\mathbf{e}}\|_{T\infty}&\le\beta_3\|\boldsymbol{\varepsilon}\|_{T\infty}+\gamma_3\|\boldsymbol{\tau}_s\|_{T\infty}+\eta_3\|\ddot{\boldsymbol{\theta}}_{des}\|_{T\infty}+\rho_3\\ \|\tilde{\mathbf{e}}_I\|_{T\infty}&\le\beta_4\|\boldsymbol{\varepsilon}\|_{T\infty}+\gamma_4\|\boldsymbol{\tau}_s\|_{T\infty}+\eta_4\|\boldsymbol{\theta}_{des}\|_{T\infty}+\rho_4\\ \|\tilde{\mathbf{e}}\|_{T\infty}&\le\beta_5\|\boldsymbol{\varepsilon}\|_{T\infty}+\gamma_5\|\boldsymbol{\tau}_s\|_{T\infty}+\eta_5\|\boldsymbol{\theta}_{des}\|_{T\infty}+\rho_5\\ \|\tilde{\dot{\mathbf{e}}}\|_{T\infty}&\le\beta_6\|\boldsymbol{\varepsilon}\|_{T\infty}+\gamma_6\|\boldsymbol{\tau}_s\|_{T\infty}+\eta_6\|\boldsymbol{\theta}_{des}\|_{T\infty}+\rho_6 \end{aligned} \quad , \quad (18)$$

where $\mathbf{e}_I$ is the time integral of error. β_i, γ_i, η_i are L_∞^n gains of operator $\mathbf{H}_i,\mathbf{G}_i,\mathbf{R}_i$ ($i=1\cdots6$) and $\mathbf{H}_i,\mathbf{G}_i$ and $\mathbf{R}_i$ are operators as below.

$$\begin{array}{lll} \mathbf{H}_1:\boldsymbol{\varepsilon}\mapsto\mathbf{e} & \mathbf{G}_1:\boldsymbol{\tau}_s\mapsto\mathbf{e} & \mathbf{R}_1:\boldsymbol{\theta}_{des}\mapsto\mathbf{e}\\ \mathbf{H}_2:\boldsymbol{\varepsilon}\mapsto\dot{\mathbf{e}} & \mathbf{G}_2:\boldsymbol{\tau}_s\mapsto\dot{\mathbf{e}} & \mathbf{R}_2:\dot{\boldsymbol{\theta}}_{des}\mapsto\dot{\mathbf{e}}\\ \mathbf{H}_3:\boldsymbol{\varepsilon}\mapsto\ddot{\mathbf{e}} & \mathbf{G}_3:\boldsymbol{\tau}_s\mapsto\ddot{\mathbf{e}} & \mathbf{R}_3:\ddot{\boldsymbol{\theta}}_{des}\mapsto\ddot{\mathbf{e}}\\ \mathbf{H}_4:\boldsymbol{\varepsilon}\mapsto\tilde{\mathbf{e}}_I & \mathbf{G}_4:\boldsymbol{\tau}_s\mapsto\tilde{\mathbf{e}}_I & \mathbf{R}_4:\boldsymbol{\theta}_{des}\mapsto\tilde{\mathbf{e}}_I\\ \mathbf{H}_5:\boldsymbol{\varepsilon}\mapsto\tilde{\mathbf{e}} & \mathbf{G}_5:\boldsymbol{\tau}_s\mapsto\tilde{\mathbf{e}} & \mathbf{R}_5:\boldsymbol{\theta}_{des}\mapsto\tilde{\mathbf{e}}\\ \mathbf{H}_6:\boldsymbol{\varepsilon}\mapsto\tilde{\dot{\mathbf{e}}} & \mathbf{G}_6:\boldsymbol{\tau}_s\mapsto\tilde{\dot{\mathbf{e}}} & \mathbf{R}_6:\boldsymbol{\theta}_{des}\mapsto\tilde{\dot{\mathbf{e}}} \end{array} \quad (19)$$

ρ_i ($i=1\cdots6$) is a constant related to the initial condition of errors. L_∞ gain of SISO linear operator P_{ii} is defined as $\int_0^\infty\|p_{ii}(\tau)\|_{i2}d\tau$ where $p_{ii}(\tau)$ is an impulse response of the system. In MIMO case, L_∞^n gain of an operator $\mathbf{P}$ is defined as $\int_0^\infty\|\mathbf{P}(\tau)\|_{i2}d\tau$ where $\left(\mathbf{P}(\tau)\right)_{ii}=p_{ii}(\tau)^2$.

Proof of Lemma 1: First, we can obtain stable transfer function matrices between the error and ε, the error and external torque, and the error and desired trajectory by using proper control gains. Then, it can be said that initial condition related parts exponentially converge and are bounded. Second, the stable transfer function has finite L_∞^n gains β_i, γ_i, η_i ($i=1\cdots6$). Thus (18) is obtained.

3.3 ε- L_∞^n Norm Bound

In this section, L_∞^n upper bound of $\boldsymbol{\varepsilon}$ is derived based on the grouping in table 1. The analysis for the free space case of group 1 is presented first.

Substituting (2), (12) and (15) into (16) yields the following equation[3] (Hsia, and Gao, 1990).

$$\begin{aligned} \boldsymbol{\varepsilon}(t)=&(\mathbf{I}-\mathbf{M}^{-1}(t)\bar{\mathbf{M}})\tilde{\mathbf{u}}(t)+(\mathbf{I}-\mathbf{M}^{-1}(t)\bar{\mathbf{M}})\boldsymbol{\varepsilon}(t-L)\\ &+\mathbf{M}^{-1}(t)\Big[\tilde{\mathbf{M}}(t)\left(-\ddot{\mathbf{e}}(t-L)+\ddot{\boldsymbol{\theta}}_{des}(t-L)\right)\\ &+\tilde{\mathbf{V}}(t)+\tilde{\mathbf{G}}(t)+\tilde{\boldsymbol{\tau}}_s(t)\Big] \end{aligned} \quad (20)$$

For derivation of Lemma 2-1 and 2-2, new variables are defined as follow.

$$\begin{array}{ll} \boldsymbol{\Delta}\triangleq\mathbf{I}-\mathbf{M}^{-1}(t)\bar{\mathbf{M}}, & \tilde{\mathbf{M}}(t)=\mathbf{M}(t)-\mathbf{M}(t-L),\\ \mathbf{Q}(t)=\mathbf{V}(t)+\mathbf{d}(t), & \tilde{\mathbf{Q}}(t)=\mathbf{Q}(t)-\mathbf{Q}(t-L). \end{array} \quad (21)$$

During the infinitesimally short time interval of collision, the joint position of a robotic system remains unchanged and joint velocities are finite (Pagilla, and Yu, 2001; Walker, 1999). Accordingly, Coriolis and centrifugal terms remain finite upon impact. Thus $\tilde{\mathbf{Q}}(t)$ is bounded.

Lemma 2-1. ε- L_∞^n Norm Bound Inequality (Free space case): In the case of n degree of freedom robot under NAC/TDC in free space, if the desired trajectory and its derivatives are in L_∞^n space and the time difference of uncertainty including disturbance is also in L_∞^n space, i.e., $\boldsymbol{\theta}_{des}(t),\dot{\boldsymbol{\theta}}_{des}(t),\ddot{\boldsymbol{\theta}}_{des}(t)\in L_\infty^n$ and $\tilde{\mathbf{w}}\in L_\infty^n$, then the following inequality can be obtained.

$$\left(1-\mu-\delta_1\beta_4-\delta_2\beta_5-\delta_3\beta_6-\delta_4\beta_1-\delta_5\beta_2-\delta_6\beta_3\right)\|\varepsilon\|_{T\infty}\le\psi_{G1},$$

where

$$\begin{aligned} \mu&=\big\|\|\boldsymbol{\Delta}\|_{i2}\big\|_\infty\\ \delta_1&=\left\|\boldsymbol{\Delta}M_s^{-1}\mathbf{G}_v\mathbf{K}_{des}\right\|_\infty\\ \delta_2&=\Big\|\left\|\boldsymbol{\Delta}\left(\mathbf{G}_v\mathbf{M}_s^{-1}\mathbf{B}_{des}+\mathbf{K}_{des}-\mathbf{c}_r\right)+\mathbf{M}^{-1}(t)\mathbf{q}_2(t)\right\|_{i2}\Big\|_\infty\\ \delta_3&=\Big\|\left\|\boldsymbol{\Delta}\left(\mathbf{G}_v+\mathbf{B}_{des}\right)+\mathbf{M}^{-1}(t)\mathbf{q}_1(t)\right\|_{i2}\Big\|_\infty\\ \delta_4&=\Big\|\left\|\mathbf{M}^{-1}(t)\tilde{\mathbf{q}}_2(t)\right\|_{i2}\Big\|_\infty\\ \delta_5&=\Big\|\left\|\mathbf{M}^{-1}(t)\tilde{\mathbf{q}}_1(t)\right\|_{i2}\Big\|_\infty\\ \delta_6&=\Big\|\left\|\mathbf{M}^{-1}(t)\tilde{\mathbf{M}}(t)\right\|_{i2}\Big\|_\infty\\ \psi_{G1}&=\Big\|\boldsymbol{\Delta}\mathbf{c}_r\tilde{\boldsymbol{\theta}}_{des}(t)-\boldsymbol{\Delta}\mathbf{G}_v\tilde{\dot{\boldsymbol{\theta}}}_{des}(t)\\ &\quad+\mathbf{M}^{-1}(t)\left(\tilde{\mathbf{M}}(t)\ddot{\boldsymbol{\theta}}_{des}(t-L)+\tilde{\mathbf{Q}}_d(t)+\tilde{\mathbf{G}}(t)+\tilde{\mathbf{w}}(t)\right)\Big\|_\infty\\ &\quad+\delta_1\left(\eta_4\|\boldsymbol{\theta}_{des}(t)\|_{T\infty}+\rho_4\right)+\delta_2\left(\eta_5\|\boldsymbol{\theta}_{des}(t)\|_{T\infty}+\rho_5\right)\\ &\quad+\delta_3\left(\eta_6\|\dot{\boldsymbol{\theta}}_{des}(t)\|_{T\infty}+\rho_6\right)+\delta_4\left(\eta_1\|\boldsymbol{\theta}_{des}(t)\|_{T\infty}+\rho_1\right) \end{aligned}$$

---

[1] $\|\bullet\|_{T\infty}$ denotes truncated L_∞^n norm of $\bullet(t)$.

[2] $\|\bullet\|_{i2}$ denotes induced 2 norm.

[3] $\tilde{\bullet}$ denotes $\bullet(t)-\bullet(t-L)$.

$$+\delta_5\left(\eta_2\left\|\dot{\boldsymbol{\theta}}_{\mathbf{des}}(t)\right\|_{T\infty}+\rho_2\right)+\delta_6\left(\eta_3\left\|\ddot{\boldsymbol{\theta}}_{\mathbf{des}}(t)\right\|_{T\infty}+\rho_3\right) \quad (22)$$

$\mathbf{Q}_{\mathbf{d}}(t)=\mathbf{Q}(\boldsymbol{\theta}_{\mathbf{des}}(t),\dot{\boldsymbol{\theta}}_{\mathbf{des}}(t))$ and $\mathbf{q}_1(t),\mathbf{q}_2(t)\in\Re^{n\times n}$ are bounded functions of time. $\mathbf{w}\in\Re^n$ is uncertainty including disturbance.

Proof of Lemma 2-1: The symbol $\boldsymbol{\Delta},\mathbf{M}(t)\in\Re^{n\times n}$ and $\mathbf{G}(t)\in\Re^n$ are sine and/or cosine functions of joint angles and thus they are bounded. $\tilde{\mathbf{M}}\in\Re^{n\times n}$ and $\tilde{\mathbf{G}}\in\Re^n$ are also bounded because they are the difference of bounded functions between time t and t-L. $\mathbf{Q}(t)$ can be written as follows.

$$\mathbf{Q}(\boldsymbol{\theta}(t),\dot{\boldsymbol{\theta}}(t))=\mathbf{Q}_{\mathbf{d}}(t)+\mathbf{O}_{\mathbf{q}}\left(\mathbf{e}(t),\dot{\mathbf{e}}(t)\right) \quad (23)$$

And we make the following assumption (Spong, and vidyasagar, 1987; Jung, *et al*., 2004).

$$\mathbf{O}_{\mathbf{q}}\left(\mathbf{e}(t),\dot{\mathbf{e}}(t)\right)\cong\mathbf{q}_1(t)\dot{\mathbf{e}}(t)+\mathbf{q}_2(t)\mathbf{e}(t)+\mathbf{w}(t) \quad (24)$$

where $\mathbf{w}\in\Re^n$ is disturbance. In the case of L_2 space analysis, semiglobal stability is proved by using this assumption (Kang, *et al*., 2004)[4]. In this case, we can only show stability, a weak version of previous one. But L_∞ analysis is practical because it includes persistent disturbance.

Substituting (12), (13), (21) and (24) into (20) yields the following.

$$\begin{aligned}\boldsymbol{\varepsilon}(t)&=\boldsymbol{\Delta}\boldsymbol{\varepsilon}(t-L)+\mathbf{G}_{\mathbf{v}}\mathbf{M}_{\mathbf{s}}^{-1}\mathbf{K}_{\mathbf{des}}\tilde{\mathbf{e}}_I(t)\\&+\left(\boldsymbol{\Delta}\left(\mathbf{G}_{\mathbf{v}}\mathbf{M}_{\mathbf{s}}^{-1}\mathbf{B}_{\mathbf{des}}+\mathbf{K}_{\mathbf{des}}-\mathbf{c}_{\mathbf{r}}\right)+\mathbf{M}^{-1}(t)\mathbf{q}_2(t)\right)\tilde{\mathbf{e}}(t)\\&+\left(\boldsymbol{\Delta}\left(\mathbf{G}_{\mathbf{v}}+\mathbf{B}_{\mathbf{des}}\right)+\mathbf{M}^{-1}(t)\mathbf{q}_1(t)\right)\dot{\tilde{\mathbf{e}}}(t)\\&+\left(\mathbf{M}^{-1}(t)\tilde{\mathbf{q}}_2\right)\mathbf{e}(t-L)+\left(\mathbf{M}^{-1}(t)\tilde{\mathbf{q}}_1\right)\dot{\mathbf{e}}(t-L)\\&-\left(\mathbf{M}^{-1}(t)\tilde{\mathbf{M}}(t)\right)\ddot{\mathbf{e}}(t-L)+\boldsymbol{\Delta}\mathbf{c}_{\mathbf{r}}\tilde{\boldsymbol{\theta}}_{\mathbf{des}}(t)-\boldsymbol{\Delta}\mathbf{G}_{\mathbf{v}}\dot{\tilde{\boldsymbol{\theta}}}_{\mathbf{des}}(t)\\&+\mathbf{M}^{-1}(t)(\tilde{\mathbf{M}}(t)\ddot{\boldsymbol{\theta}}_{\mathbf{d}}(t-L)+\tilde{\mathbf{Q}}_{\mathbf{d}}(t)+\tilde{\mathbf{G}}(t)+\tilde{\mathbf{w}}(t))\end{aligned} \quad (25)$$

Take norms of both sides of (25). Define each term μ_{G1} and $\delta_{i\_G1}(i=1\cdots6)$ as in (22), and ψ_{1_G1} as below.

$$\begin{aligned}\psi_{1\_G1}=&\Big\|\boldsymbol{\Delta}\mathbf{c}_{\mathbf{r}}\tilde{\boldsymbol{\theta}}_{\mathbf{des}}(t)-\boldsymbol{\Delta}\mathbf{G}_{\mathbf{v}}\dot{\tilde{\boldsymbol{\theta}}}_{\mathbf{des}}(t)\\&+\mathbf{M}^{-1}(t)(\tilde{\mathbf{M}}(t)\ddot{\boldsymbol{\theta}}_{\mathbf{d}}(t-L)+\tilde{\mathbf{Q}}_{\mathbf{d}}(t)+\tilde{\mathbf{G}}(t)+\tilde{\mathbf{w}}(t))\Big\|_\infty\end{aligned} \quad (26)$$

Then we can derive the following inequality.

$$\begin{aligned}\|\boldsymbol{\varepsilon}(t)\|_{T\infty}\le&\Big(\mu\|\boldsymbol{\varepsilon}(t-L)\|_{T\infty}+\delta_1\|\tilde{\mathbf{e}}_{\mathbf{I}}(t)\|_{T\infty}+\delta_2\|\tilde{\mathbf{e}}(t)\|_{T\infty}\\&+\delta_3\left\|\dot{\tilde{\mathbf{e}}}(t)\right\|_{T\infty}+\delta_4\|\mathbf{e}(t-L)\|_{T\infty}+\delta_5\|\dot{\mathbf{e}}(t-L)\|_{T\infty}\\&+\delta_6\|\ddot{\mathbf{e}}(t-L)\|_{T\infty}+\psi_{1\_G1}\Big)\end{aligned} \quad (27)$$

From (22) and Lemma 1, we get [5]

$$\begin{aligned}\|\boldsymbol{\varepsilon}(t)\|_{T\infty}\le&\mu\|\boldsymbol{\varepsilon}(t)\|_{T\infty}+\delta_1\beta_4\|\boldsymbol{\varepsilon}(t)\|_{T\infty}+\delta_2\beta_5\|\boldsymbol{\varepsilon}(t)\|_{T\infty}\\&+\delta_3\beta_6\|\boldsymbol{\varepsilon}(t)\|_{T\infty}+\delta_4\beta_1\|\boldsymbol{\varepsilon}(t)\|_{T\infty}+\delta_5\beta_2\|\boldsymbol{\varepsilon}(t)\|_{T\infty}\\&+\delta_6\beta_3\|\boldsymbol{\varepsilon}(t)\|_{T\infty}+\psi_{G1}\end{aligned} \quad (28)$$

Rearranging (28) leads to,

$$(1-\mu-\delta_1\beta_4-\delta_2\beta_5-\delta_3\beta_6-\delta_4\beta_1-\delta_5\beta_2-\delta_6\beta_3)\|\boldsymbol{\varepsilon}(t)\|_{T\infty}\le\psi_{G1}. \quad (29)$$

Note that ψ_{1_G1} and ψ_{G1} consist of bounded values. Similarly, for the constrained space case of group 2 Lemma 2-2 can be obtained as below. Its derivation is shown in Appendix. The only difference is that there exists an external force in the constrained space case.

Lemma 2-2. ε- L_∞^n Norm Bound Inequality (Constrained Space Case): In the case of n degree of freedom robot under NAC/TDC in constrained space, if the desired trajectory and its derivatives are in L_∞^n space and the external force and the time difference of uncertainty including disturbance are also in L_∞^n space, i.e., $\boldsymbol{\theta}_{\mathbf{des}}(t)\in L_\infty^n$, $\dot{\boldsymbol{\theta}}_{\mathbf{des}}(t)\in L_\infty^n$, $\ddot{\boldsymbol{\theta}}_{\mathbf{des}}(t)\in L_\infty^n$, $\boldsymbol{\tau}_{\mathbf{s}}\in L_\infty^n$ and $\tilde{\mathbf{w}}\in L_\infty^n$, then the following inequality can be obtained.

$$(1-\mu-\delta_1\beta_4-\delta_2\beta_5-\delta_3\beta_6-\delta_4\beta_1-\delta_5\beta_2-\delta_6\beta_3)\|\boldsymbol{\varepsilon}(t)\|_{T\infty}\le\psi_{G2},$$

where

$$\begin{aligned}\psi_{G2}=&\Big\|\boldsymbol{\Delta}\mathbf{c}_{\mathbf{r}}\tilde{\boldsymbol{\theta}}_{\mathbf{des}}(t)-\boldsymbol{\Delta}\mathbf{G}_{\mathbf{v}}\dot{\tilde{\boldsymbol{\theta}}}_{\mathbf{des}}(t)+\mathbf{M}^{-1}(t)\tilde{\mathbf{M}}(t)\ddot{\boldsymbol{\theta}}(t-L)\\&+\mathbf{M}^{-1}(t)(\tilde{\mathbf{Q}}_{\mathbf{d}}(t)+\tilde{\mathbf{G}}(t)+\tilde{\mathbf{w}}(t))+\boldsymbol{\Delta}\mathbf{G}_{\mathbf{v}}\mathbf{M}_{\mathbf{s}}^{-1}\int_{t-L}^{t}\boldsymbol{\tau}_{\mathbf{s}}(\sigma)d\sigma\\&+\mathbf{M}^{-1}(t)\tilde{\boldsymbol{\tau}}_{\mathbf{s}}(t)\Big\|_\infty+\delta_1\left(\eta_4\|\boldsymbol{\theta}_{\mathbf{des}}(t)\|_{T\infty}+\gamma_4\|\boldsymbol{\tau}_{\mathbf{s}}(t)\|_{T\infty}+\rho_4\right)\\&+\delta_2\left(\eta_5\|\boldsymbol{\theta}_{\mathbf{des}}(t)\|_{T\infty}+\gamma_5\|\boldsymbol{\tau}_{\mathbf{s}}(t)\|_{T\infty}+\rho_5\right)+\delta_3\Big(\eta_6\left\|\dot{\boldsymbol{\theta}}_{\mathbf{des}}(t)\right\|_{T\infty}\\&+\gamma_6\|\boldsymbol{\tau}_{\mathbf{s}}(t)\|_{T\infty}+\rho_6\Big)+\delta_4\left(\eta_1\|\boldsymbol{\theta}_{\mathbf{des}}(t)\|_{T\infty}+\gamma_1\|\boldsymbol{\tau}_{\mathbf{s}}(t)\|_{T\infty}+\rho_1\right)\\&+\delta_5\left(\eta_2\left\|\dot{\boldsymbol{\theta}}_{\mathbf{des}}(t)\right\|_{T\infty}+\gamma_2\|\boldsymbol{\tau}_{\mathbf{s}}(t)\|_{T\infty}+\rho_2\right)+\delta_6\Big(\eta_3\left\|\ddot{\boldsymbol{\theta}}_{\mathbf{des}}(t)\right\|_{T\infty}\\&+\gamma_3\|\boldsymbol{\tau}_{\mathbf{s}}(t)\|_{T\infty}+\rho_3\Big)\end{aligned} \quad .(30)$$

3.4 *Sufficient Stability Conditions for NBBIC*

We have shown the inequalities of $\|\boldsymbol{\varepsilon}(t)\|_{T\infty}$ by Lemma 2-1 and Lemma 2-2. The sufficient condition for these inequalities to have upper bounds are shown below.

$$\mu+\delta_1\beta_4+\delta_2\beta_5+\delta_3\beta_6+\delta_4\beta_1+\delta_5\beta_2+\delta_6\beta_3<1 \quad (31)$$

If (31) holds, $\|\boldsymbol{\varepsilon}(t)\|_\infty$ has an upper bound because all terms of (31) are not related to T, which is a symbol of truncated norm. The fact that $\|\boldsymbol{\varepsilon}(t)\|_\infty$ can have an upper bound means that the time-delay estimation error $\boldsymbol{\varepsilon}(t)$ of (15) can be bounded. Therefore, in the case of group 1 and group 2, stability can be guaranteed if we set control gains to satisfy (31). In the case of group 3, a robot is passive since there is no control input applied to it; hence, the system is stable (Ortega, and Spong, 1988). Therefore, we can obtain the following stability theorem for the nonlinear bang-bang impact control from Lemma 1, 2-1 and 2-2.

***NBBIC Stability Theorem*:** The sufficient conditions for stability under the nonlinear bang-bang impact control become:

$$\mu+\delta_1\beta_4+\delta_2\beta_5+\delta_3\beta_6+\delta_4\beta_1+\delta_5\beta_2+\delta_6\beta_3<1$$

3.5 *Physical Implication of NBBIC Stability Condition*

In order to understand the physical implication of NBBIC stability theorem, we substitute the norm values of (22) for free space case and of (30) for constrained space case into (31). Then we get,

$$\left\|\left\|\mathbf{I}-\mathbf{M}^{-1}\bar{\mathbf{M}}\right\|_{i2}\right\|_\infty<\frac{(1-c)}{1+\left(\beta_4\kappa_1+\beta_5\kappa_2+\beta_6\kappa_3\right)}, \quad (32)$$

where

$\kappa_1=\left\|M_s^{-1}\mathbf{G}_{\mathbf{v}}\mathbf{K}_{\mathbf{des}}\right\|_{i2}$

$\kappa_2=\left\|\left(M_s^{-1}\mathbf{G}_{\mathbf{v}}\mathbf{B}_{\mathbf{des}}+\mathbf{K}_{\mathbf{des}}-\mathbf{c}_{\mathbf{r}}\right)\right\|_{i2}$

$\kappa_3=\left\|\left(\mathbf{G}_{\mathbf{v}}+\mathbf{B}_{\mathbf{des}}\right)\right\|_{i2}$

$c=\beta_5\left\|\left\|\mathbf{M}^{-1}(t)\mathbf{q}_2(t)\right\|_{i2}\right\|_\infty+\beta_6\left\|\left\|\mathbf{M}^{-1}(t)\mathbf{q}_1(t)\right\|_{i2}\right\|_\infty+\beta_1\left\|\left\|\mathbf{M}^{-1}(t)\tilde{\mathbf{q}}_2(t)\right\|_{i2}\right\|_\infty$

---

[4] Semiglobal stability is a kind of asymptotic stability.

[5] $\|\bullet(t-L)\|_{T\infty}\le\|\bullet(t)\|_{T\infty}$ is always established.

$$+\beta_2\left\|\left\|\mathbf{M}^{-1}(t)\tilde{\mathbf{q}}_1(t)\right\|_{i2}\right\|_\infty+\beta_3\left\|\left\|\mathbf{M}^{-1}(t)\tilde{\mathbf{M}}(t)\right\|_{i2}\right\|_\infty . \quad (33)$$

Note that c in (33) is composed of the differences of bounded values such as $\tilde{\mathbf{M}}, \tilde{\mathbf{q}}_1$, and $\tilde{\mathbf{q}}_2$ and the bounded values multiplied by small values β_5 and β_6 which are the time integral of difference of impulse response matrix for stable linear system. Therefore, c is negligible during the impact and constrained motion when there is not much change in Coriolis and centrifugal forces between time t and t-L (Pagilla, and Yu, 2001; Walker, 1999). However, c is not negligible during a certain constrained motion which involves significant changes in these state dependent forces between time t and t-L.

When these terms are negligible, NBBIC is always stable if $\bar{\mathbf{M}}=\mathbf{M}$ since it makes the left hand side of (32) zero. In reality, however, it is difficult to estimate robot inertia $\mathbf{M}$ accurately. When the inertia estimate $\bar{\mathbf{M}}$ differs from the actual inertia $\mathbf{M}$, the stable range of $\bar{\mathbf{M}}$ is determined by the delay time L and control gains. It can be deduced from (32) that the more $\bar{\mathbf{M}}$ differs from $\mathbf{M}$, the smaller L should be to achieve stability. It is noted that the system under NBBIC is stable regardless of controller gains if the estimation of inertia is accurate and a delay time L is small. It is a natural conclusion because the NAC is designed to observe the passivity constraint. However, as the degrees of freedom of a robot increases, it becomes more difficult to obtain accurate estimation of robot inertia.

When there are significant changes in Coriolis and centrifugal forces between time t and t-L, i.e., c is not negligible as in free space and a certain constrained motion, it imposes more strict constraints on the range of $\bar{\mathbf{M}}$ and L. For example, if a robot under NBBIC approaches an environment from free space to perform a contact task on a fixed stiff wall, the stability condition for free space motion is more difficult to satisfy than that of such constrained motion. It was confirmed by experiments. Our experiments demonstrate that the nonlinear bang-bang impact controller can make stable contact with a stiff environment without changing gains by using gains set for stable free space motion (Lee, *et al.*, 2003a, b). It shows that if the controller gains make stable free space motion, they can also make stable constrained space motion which experiences less change in Coriolis and centrifugal forces than those in free space.

4. EXPERIMENT

In this section, experiments are performed to verify the NBBIC stability theorem derived in Section 3.

Experiments are performed to verify the proposed stability criterion by using SCARA type two D.O.F. robot with sampling time L=1msec (fig. 1).

First, one D.O.F experiment is conducted using only the 2nd axis of the robot. The objective is to drive robot 0.0746m with desired velocity of 0.1865m/s, i.e., 0.0728m in free space and 0.0018m after contact with silicon wall. The theoretical stable range of the inertia estimate $\bar{M}$ is $0.015\ kg\cdot m^2 \le \bar{M} \le 0.135\ kg\cdot m^2$ with M_s=0.07 kg·m^2, G_v=6 N·m/s, B_{des}=30 N·m/s, and K_{des}=140 N·m. The experimental results in fig.2 show that stable response is obtained with lower stability bound. But, the stable upper bound of $\bar{M}$ is observed to be 0.036 kg·m^2. Second, two D.O.F. experiments are performed with the same stable gains used for the one D.O.F. experiments. $\bar{\mathbf{M}}$ is selected as a constant diagonal matrix ($diag[\alpha_1,\alpha_2]$) and the maximum stable gain of $\alpha_2=0.030\ \mathrm{kg\cdot m^2}$ is used. With these values, the theoretical stable range of α_1 is $0.34\ \mathrm{kg\cdot m^2}\le\alpha_1\le 0.82\ \mathrm{kg\cdot m^2}$. The lower bound of 0.34 kg·m^2 produces stable response as shown in fig.3. However, it is observed that the maximum stable upper bound is 0.5 kg·m^2 instead of 0.82 kg·m^2. It appears that the stable upper bound is limited by noise effect due to acceleration signals and etc. If we employ a first order digital low pass filter with the cutoff frequency λ to cancel noise, control input changes accordingly as below (Youcef-Toumi, and Wu, 1992)

$$\boldsymbol{\tau}(t)=\bar{\mathbf{M}}(\mathbf{u}(t)-\ddot{\boldsymbol{\theta}}(t-L))+\boldsymbol{\tau}'(t-L), \quad (34)$$

$$\boldsymbol{\tau}'(t)=\frac{\lambda'}{1+\lambda'}\boldsymbol{\tau}(t)+\frac{1}{1+\lambda'}\boldsymbol{\tau}'(t-L) \quad (\lambda'=\lambda L), \quad (35)$$

where $\boldsymbol{\tau}$ is the input to the filter and $\boldsymbol{\tau}'$ is the outputfrom the filter. Substituting (34) into (35) leads to the following control input

$$\boldsymbol{\tau}'(t)=\frac{\lambda'}{1+\lambda'}\bar{\mathbf{M}}(\mathbf{u}(t)-\ddot{\boldsymbol{\theta}}(t-L))+\boldsymbol{\tau}'(t-L) \quad (36)$$

Thus the use of a first order digital low pass filter has the same effect as lowering $\bar{\mathbf{M}}$. The noise effect is more pronounced with higher gains of $\bar{\mathbf{M}}$ since they excite high frequency dynamics of robots. That is the reason why the stable upper bound is lower than the theoretical one. If the original upper bound of $\bar{\mathbf{M}}$ which is calculated from equation (32)is $\bar{\mathbf{M}}_{max}$ and dominant noise frequency of ith joint is λ_i, then the revised upper bound($\bar{\mathbf{M}}'_{max}$) becomes:

$$\bar{\mathbf{M}}'_{max}=\left(diag\left(\frac{\lambda_1 L}{1+\lambda_1 L}, \ \cdots \ , \frac{\lambda_n L}{1+\lambda_n L}\right)\right)\bar{\mathbf{M}}_{max} \quad (37)$$

We examine the noise effect of acceleration signal on overall performance of NBBIC. The Laplace transform of NAC/TDC control input of (34) without using low-pass filter is

$$\boldsymbol{\tau}(s)=\bar{\mathbf{M}}\left\{\mathbf{u}(s)-s^2e^{-Ls}\boldsymbol{\theta}(s)\right\}+e^{-Ls}\boldsymbol{\tau}(s) . \quad (38)$$

After some manipulation the following equation is obtained.

$$\boldsymbol{\tau}(s)=\frac{1}{\left(1-e^{-Ls}\right)}\bar{\mathbf{M}}\left\{\mathbf{u}(s)-s^2e^{-Ls}\boldsymbol{\theta}(s)\right\} . \quad (39)$$

When L is small, the following approximation can be used (by Taylor expansion)

$$\left(1-e^{-Ls}\right)\approx Ls \ . \quad (40)$$

Inserting (39) into (38) yields

$$\boldsymbol{\tau}(s)\cong\frac{1}{Ls}\bar{\mathbf{M}}\left(\mathbf{u}(s)-s^2e^{-Ls}\boldsymbol{\theta}(s)\right) . \quad (41)$$

Likewise, in discrete time domain, it can be shown that the acceleration signal is accumulated to become approximately equivalent to a velocity signal as below.

Figure 1. SCARA Robot Experimental setup

$$\begin{aligned}\boldsymbol{\tau}(k) &= \bar{\mathbf{M}}\left(\mathbf{u}(k)-\ddot{\boldsymbol{\theta}}(k\text{-}1)\right)+\boldsymbol{\tau}(k\text{-}1) \\ &= \bar{\mathbf{M}}\left(\mathbf{u}(k)\text{-}\ddot{\boldsymbol{\theta}}(k\text{-}1)+\mathbf{u}(k\text{-}1)\text{-}\bar{\mathbf{M}}\ddot{\boldsymbol{\theta}}(k\text{-}2)\right)+\boldsymbol{\tau}(k\text{-}2) \\ &\cdots \\ &= \bar{\mathbf{M}}\sum_{j=0}^{k}\mathbf{u}(j)\text{-}\bar{\mathbf{M}}\sum_{j=0}^{k}\ddot{\boldsymbol{\theta}}(j\text{-}1)\end{aligned} \quad .(42)$$

Equations (40) and (41) show that the acceleration term is integrated/accumulated over to the last sampling time, that is, an acceleration term becomes in fact a velocity term when NAC/TDC is actually implemented. It is as if the acceleration signal is low-pass-filtered as shown in (40). Therefore, it can be said that the noise effect of acceleration signals does not seriously affect the overall performance of NAC/TDC even though it reduces the stability bounds.

5. CONCLUSION

In this paper, we derived sufficient stability conditions for the nonlinear bang-bang impact control based on L_{∞}^{n} space analysis. The stability condition has a concise form and gives straightforward physical insight. The analysis shows that when the inertia estimate $\bar{\mathbf{M}}$ differs from the actual inertia $\mathbf{M}$, the stable range of $\bar{\mathbf{M}}$ is determined by a delay time L and control gains. It also shows that it is more difficult to achieve stability in free space than in a certain constrained motion, which does not involve significant changes in Coriolis and centrifugal forces between time t and $t\text{-}L$. Experimental results validate the sufficient stability conditions. Experiments show that the stability conditions are not stringent allowing a broad range of gains and parameter estimation errors. In reality, however, experimental noises reduce the stability region and it is more apparent as the order of systems increases. NBBIC can be used for robot interactions with unknown physical environments such as robots in space exploration, cooperative robot tasks and mobile robots. NBBIC can also be used for micro/nano manipulations using an atomic force microscope, where real time vision is unavailable during contact manipulation without an additional vision system.

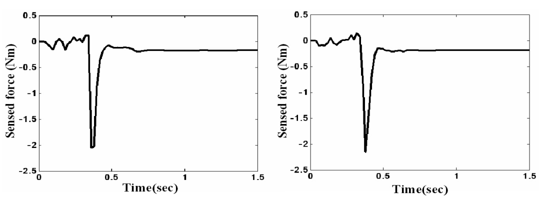

(a) $\bar{M}=0.013\ \mathrm{kg}\cdot\mathrm{m}^2$ (b) $\bar{M}=0.036\ \mathrm{kg}\cdot\mathrm{m}^2$

Figure 2. Contact force (one D.O.F)

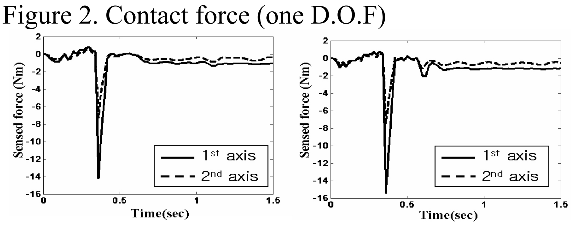

(a) $\alpha_1 = 0.34\ \mathrm{kg}\cdot\mathrm{m}^2$ (b) $\alpha_1 = 0.5\ \mathrm{kg}\cdot\mathrm{m}^2$

Figure 3. Contact force (two D.O.F)

REFERENCES

Hsia, T. C. and Gao, L. S. (1990). Robot manipulator control using decentralized linear time-invariant time-delayed joint controllers, *IEEE Int. Conf. on Robot and Automat.* (ICRA), Cincinnati, Ohio, pp. 2070-2075.

Indri, M. and Tornambe, A. (1999). Impact model and control of two multi-DOF cooperating manipulators, *IEEE Trans. on Automatic Control*, **vol. 44**, No. 6, pp. 1528 – 1533

Jung, J.H., Chang, P.H. and Kwon, O.S. (2004). A new stability analysis of time delay control for input-output linearizable plants, *American Contr. Conf.* (ACC), Boston, MA, pp.4972-4979

Kang, S. H., Chang, P.H. and Lee, E (2004). Stability analysis of Nonlinear bang-bang impact control for one degree of freedom robotic manipulator, *IEEE International Conference on Mechatronics* (ICM), Istanbul, Turkey. pp.84-91

Lee, E. (1994). *Force and impact control for robot manipulators with unknown dynamics and disturbances*, Ph.D. Dissertation, Dept. of Mechanical and Aerospace Engineering, Case Western Reserve Univ., Cleveland, OH

Lee, E., Park , J., Loparo , K. A., Schrader, C. B. and Chang, P. H. (2003a). Bang-Bang impact control using hybrid impedance/time-delay control, *IEEE/ASME Trans. on Mechatronics*, **vol.8**, No.2, pp.272-277.

Lee, E., Park, J., Schrader, C.B. and Chang, P.H. (2003b). Hybrid impedance/time-delay control from free space to constrained motion, *American Contr. Conf.* (ACC), Denver, CO, pp. 2132 - 2137.

Lee, J. W., Park, J. and Chang, P.H. (1997). A systematic gain tuning of PID controller based on the concept of time delay control, *Korea Automat. Contr. Conf.* (KACC), Seoul, Korea, pp. 1093 - 1096.

Nenchev, D.N., Yoshida, K. (1999). Impact analysis and post-impact motion control issues of a free-floating Space robot subject to a force impulse, *IEEE Trans. on Robot and Automat.*, **vol.15**, pp.548 – 557.

Newman, W. S. (1992). Stability and performance limits of interaction controllers, *Trans. Of ASME, J. Dyn. Sys., Meas., Contr*, **vol.114**, pp.563-570.

Ortega, Romeo and Spong, Mark W. (1988). Adaptive motion control of rigid robots: A tutorial, *IEEE Int. Conf. on Decision and Control*(CDC), pp.1575 - 1584.

Pagilla, Prabhakar R., and Yu, Biao (2001). A stable transition controller for constrained robots, *IEEE/ASME Trans. on Mechatronics*, **vol.6**, No.1, pp.65-74.

Spong, Mark W. and Vidyasagar, M. (1987). Robust linear compensator design for nonlinear robotic control, *IEEE J. of Robotics and Automation*, **vol.RA-3**, No.4, pp.345-351.

Walker, Ian D. (1994). Impact configurations and measures for kinematically redundant and multiple armed robot systems, *IEEE Trans. on Robotics and Automation*, **vol.10**, No.5, pp.670-683.

Youcef-toumi, K. and Wu, S.-T. (1992). Input/Output linearization using time delay control, *Trnas. Of ASME, J. Dyn, Sys., Meas., Contr*, **vol. 114**, pp10-19.

Youcef-Toumi, K. and Ito, O. (1990). A time delay controller for systems with unknown dynamics, *Trans. of ASME, J. Dyn. Sys., Meas., Contr*, **vol. 112**, pp. 133-142.

Appendix

Proof of one degree of freedom system is shown in (Kang, *et al.*, 2004). For multi-degree of freedom case, proof of Lemma 2-2 and finite number of switching will be available upon request.